A&A 530, L4 (2011)
DOI: 10.1051/0004-6361/201116954

Astronomy & Astrophysics

Letter to the Editor

High resolution spectroscopy of Pluto's atmosphere: detection of the 2.3 μm CH_4 bands and evidence for carbon monoxide

E. Lellouch[1], C. de Bergh[1], B. Sicardy[1,2,⋆], H. U. Käufl[3], and A. Smette[4]

[1] LESIA, Observatoire de Paris, 5 place Jules Janssen, 92195 Meudon, France
e-mail: emmanuel.lellouch@obspm.fr
[2] Université Pierre et Marie Curie, 4 place Jussieu, 75005 Paris, France
[3] European Space Observatory, Karl-Schwarzschild-Strasse 2, 85748 Garching bei München, Germany
[4] European Space Observatory, Alonso de Córdova 3107, Casilla 19001, Vitacura, Chile

Received 24 March 2011 / Accepted 21 April 2011

ABSTRACT

Aims. The goal is to determine the composition of Pluto's atmosphere and to constrain the nature of surface-atmosphere interactions.
Methods. We perform high-resolution spectroscopic observations in the 2.33–2.36 μm range, using CRIRES at the VLT.
Results. We obtain (i) the first detection of gaseous methane in this spectral range, through lines of the $\nu_3 + \nu_4$ and $\nu_1 + \nu_4$ bands (ii) strong evidence (6-σ confidence) for gaseous CO in Pluto. For an isothermal atmosphere at 90 K, the CH_4 and CO column densities are 0.75 and 0.07 cm-am, within factors of 2 and 3, respectively. Using a physically-based thermal structure model of Pluto's atmosphere also satisfying constraints from stellar occultations, we infer CH_4 and CO mixing ratios $q_{CH_4} = 0.6^{+0.6}_{-0.3}$% (consistent with results from the 1.66 μm range) and $q_{CO} = 0.5^{+1}_{-0.25} \times 10^{-3}$. The CO atmospheric abundance is consistent with its surface abundance. As for Triton, it is probably controlled by a thin, CO-rich, detailed balancing layer resulting from seasonal transport and/or atmospheric escape.

Key words. Kuiper belt objects: individual: Pluto – infrared: general – solar system: general – infrared: solar system

1. Introduction

Along with Triton's, Pluto's tenuous atmosphere is a benchmark example of an atmosphere controlled by vapor pressure equilibrium with surface ices. Pluto's surface is dominated by N_2 ice, but other detected surface compounds include CH_4, CO and, tentatively, C_2H_6 and other non-volatile species (e.g. Cruikshank et al. 1997; Douté et al. 1999; Grundy & Buie 2001, 2002; Olkin et al. 2007; Protopapa et al. 2008; Merlin et al. 2010). Pluto's atmospheric composition remains poorly known. Based on its surface abundance and large volatility, and albeit not observed spectroscopically, N_2 is known to dominate Pluto's atmosphere. The only other gas phase species to have been detected is methane. It was first observed in its $2\nu_3$ band near 1.66 μm by Young et al. (1997), providing the first estimate of its CH_4 column density (1.2 cm-am within a factor of 3–4, assuming a gas temperature of 100 K). Much improved observations obtained with the CRIRES infrared echelle spectrograph at the VLT in 2008 (Lellouch et al. 2009), including the detection of numerous lines, up to $J = 8$, made it possible to separate temperature and abundance effects in the Pluto spectra, and to constrain the depth of Pluto's atmosphere. Assuming an isothermal atmosphere, the data indicated a mean gas temperature $T = 90^{+25}_{-18}$ K and a methane column density $a_{CH_4} = 0.75^{+0.55}_{-0.30}$ cm-am. Although Pluto's surface pressure is uncertain, the combined analysis of these data with stellar occultation curves indicated a CH_4/N_2 mixing ratio $q_{CH_4} = 0.5 \pm 0.1$%.

The other species to be expected in Pluto's atmosphere based on volatility considerations is carbon monoxide. Searches for CO have been conducted already a decade ago (Bockelée-Morvan et al. 2001; Young et al. 2001), but as detailed below, results have been relatively unconstraining. More recently (July 2009), and using again CRIRES/VLT, Lellouch et al. (2010) detected CO in Triton's atmosphere from its CO(2–0) band at 2.35 μm, with a column density of ~0.30 cm-am, corresponding to $CO/N_2 \sim 6 \times 10^{-4}$ for an estimated 40 μbar surface pressure. They also searched for CO on Pluto in the (3–0) band near 1.57 μm. The choice of that band was motivated by the much larger brightness of Pluto in H vs. K band (geometric albedo ~0.6 at 1.57 μm vs. ~0.2 at 2.35 μm). On the other hand, lines of the CO(3–0) band, whose strengths are ~2 orders of magnitude weaker than those of the (2–0) band, are expected to show up only for large CO abundances, and as a matter of fact, only an upper limit of 1 cm-am was obtained, i.e. $CO/N_2 < 5 \times 10^{-3}$ for a typical 15 μbar pressure. Based on considerations on the surface/atmosphere equilibrium and the CO surface abundance, estimates of the CO abundance on Pluto are ~10 times smaller. Reaching this sensitivity in the near-IR demands the use of CO(2–0) band, but given that Pluto is ~3.5 times fainter than Triton at 2.35 μm, this in turn requires a deep integration. We here report on such observations.

2. VLT/CRIRES observations

Spectroscopic observations of Pluto were obtained during two half-nights on July 27 (0h40–4h25 UT) and 29 (0h10–5h16 UT) 2010, using the CRIRES instrument (Käufl et al. 2004) installed on ESO VLT (European Southern Observatory Very Large Telescope) UT1 (Antu) 8.2 m telescope. We used the instrument in adaptive optics mode and with a slit of 0.4″. The spectral resolution, measured from the linewidths and the source effective size, was 60 000. We targeted a portion of the (2–0)

⋆ Senior member of the Institut Universitaire de France.

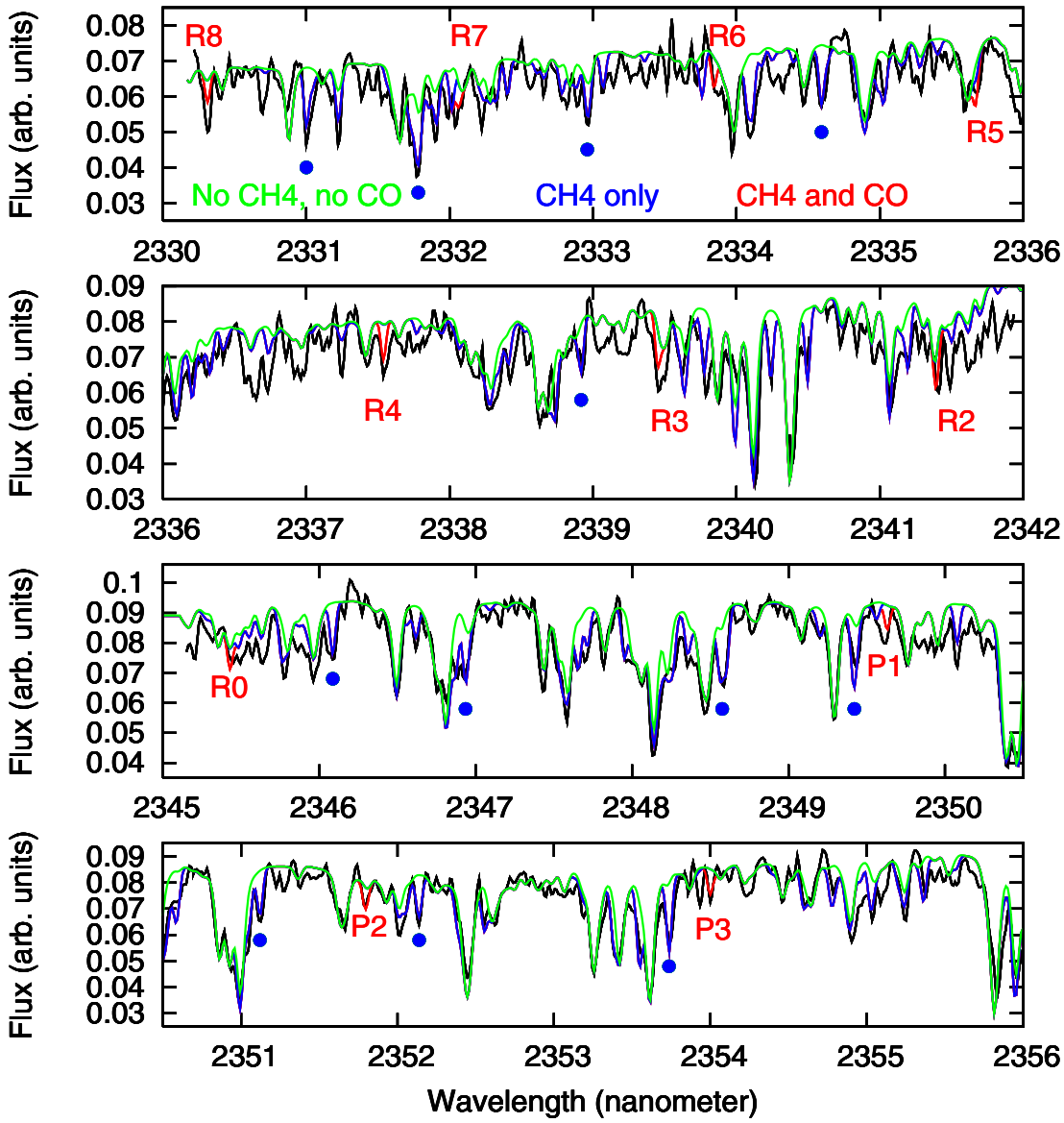

Fig. 1. Black: Pluto spectrum at 2330–2342 and 2345–2356 nm (arbitrary units). The total integration time is 7h20 min. The spectral resolution is 60 000. Red, blue and green curves show synthetic spectra for an isothermal Pluto atmosphere at $T = 90$ K, and including telluric and solar lines. Green: no methane and CO in Pluto's atmosphere. Blue: methane is included with a 0.75 cm-am column density. Red: CO is also included with a column density of 0.07 cm-am. Blue dots locate the methane features that were used in the line coaddition process shown in Fig. 2.

band of CO, also encompassing a fraction of the $\nu_1 + \nu_4$ and $\nu_3 + \nu_4$ bands of CH_4. The instrument includes four detectors. On July 27, we covered the 2312–2325, 2330–2342, 2345–2356 and 2359–2370 nm ranges. However, detectors 1 and 4 were affected by flux losses along the slit. On July 29, we used a fast ("windowed") readout mode in which only detectors 2 and 3 are read (and windowed), resulting in a noticeable gain in sensitivity for faint targets. Pluto's mean (East) longitude for the two dates was 118° and 5°, respectively. A large Doppler shift (~15.9 and ~16.7 km s^{-1} for July 27 and 29) ensured proper separation of the target Pluto lines from the telluric absorptions, particularly from CH_4. Each night we observed a telluric standard (HR 5917) to check for wavelength calibration and atmospheric transmission. All data were reduced using the standard steps of the CRIRES pipeline, including corrections for darks, flatfield, image recombination, replacement of bad pixels and outliers, and spectral extraction. Spectra from the two dates were finally coadded, providing a mean S/N of 15–20 per resolving element.

3. Modelling and evidence for CO

The total spectrum in the 2330–2342 and 2345–2356 nm ranges (Fig. 1) shows the detection of many features due to the $\nu_3 + \nu_4$ band of CH_4 (plus some lines of the $\nu_1 + \nu_4$ band longwards of 2350 nm) representing the first detection of these bands in Pluto's atmosphere. As in our previous studies (Lellouch et al. 2009, 2010) we constructed a direct, disk-integrated, line-by-line atmospheric model of Pluto, including solar lines reflected off Pluto's surface as well as the telluric transmission and accounting for the proper Doppler shifts. In a first step, we assumed a single, homogeneous layer at 90^{+25}_{-18} K, as inferred from the 1.66 μm spectrum (Lellouch et al. 2009). This yielded a best fit methane column density $a_{CH_4} = 0.75^{+1.0}_{-0.5}$ cm-am, consistent with the $2\nu_3$ inferences. Here the large error bar combines quadratically a factor-of-2 uncertainty due to the S/N limitations and a similar uncertainty due to the range in mean gas temperature. The lower precision compared to results from the 1.66 μm band is due to the lower S/N of the 2.35 μm spectrum.

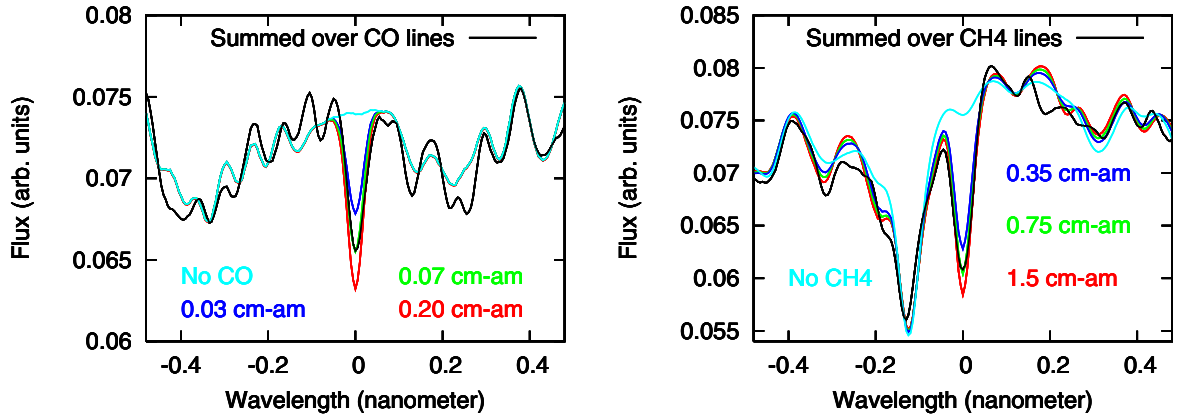

Fig. 2. Black: Coadded CO (*left*) and CH_4 (*right*) line, obtained from coaddition of the observed spectrum within ±0.5 nm of (i) the R2–R7 and P1–P3 lines of CO and (ii) the 12 CH_4 features identified by dots in Fig. 1. Colored lines: result of the same treatment applied to synthetic spectra. In *the right panel*, the feature at –0.13 nm is mostly due to the telluric counterpart of the coadded methane line.

Pluto's thermal structure is characterized by a "warm" (~100 K) upper atmosphere, a sharp inversion layer in the 3–10 μbar pressure range, and possibly but not necessarily a cold (~36–45 K) troposphere. By combining their 1.66 μm CH_4 spectrum with occultation data, Lellouch et al. (2009) found that the stratospheric gradient is in the range 3–15 K/km, the (current) surface pressure is 6.5–24 μbar, and the troposphere is at most 17 km deep. Each of the allowed thermal profiles is associated with a methane column density a_{CH_4}, required to fit the 1.66 μm spectrum. Deeper (i.e. colder) models require larger methane columns than shallower models. The range for a_{CH_4} in these models was then 0.65–1.3 cm-am, but the CH_4 mixing ratio could be accurately determined to $q_{CH_4} = 0.5 \pm 0.1\%$. We re-modelled the 2.35 μm spectrum with one "nominal" thermal profile, having a stratospheric gradient of 6 K/km, a wet tropospheric adiabat, and a surface pressure of 15 μbar, corresponding to a N_2 column density of 210 cm-am (this profile is one of the "green" profiles shown in Fig. 4 of Lellouch et al. 2009). Assuming that methane is vertically uniform, an identical fit to that shown in Fig. 1 is then obtained for $a_{CH_4} = 1.2$ cm-am, i.e. $q_{CH_4} = 0.57\%$. Refitting the data with atmospheres restricted to $p = 6.5$ μbar or extending to $p = 24$ μbar (Table 1) indicates that S/N limitations dwarf thermal profile uncertainties, and the methane mixing ratio indicated by our spectrum is $0.6^{+0.6}_{-0.3}\%$.

Besides the CH_4 features, Pluto's atmosphere spectrum shows absorptions at the positions of most of the CO(2–0) lines covered by the observed spectral range (R8–R2, R0 and P1–P3), and that are not fit by the previous methane-only model. Including CO at 90 K and with a column densityof 0.07 cm-am clearly improves the fit in the vicinity of all these lines. Admittedly, several mismatches remain, that are comparable to or sometimes even larger than the features tentatively identified as due to CO; examples occur near 2330.6, 2336.6, 2337 or 2353.9 nm. To assess the significance of the result, we coadded the data over ±0.5 nm broad intervals centered on all the CO line positions, without any a priori exclusion (except for the R0 and R8 lines that are too close to detector edge). This treatment (Fig. 2, left) produces clear evidence for an absorption line at the "zero wavelength", around which significant structure is observed. Performing the same treatment on synthetic spectra allows us to interpret this residual structure as being due to the more or less random co-addition of other lines (telluric, solar, or Pluto CH_4) in the vicinity of the CO lines. The remaining standard deviation between model and observation ($\sim 1.3 \times 10^{-3}$ in the units of Fig. 2, i.e. 1.8% of the continuum) indicates a 6-σ detection of the "combined CO line". For an isothermal 90 K atmosphere, the best fit is achieved for a CO column density $a_{CO} = 0.07$ cm-am. For the above nominal thermal profile, it is obtained for $a_{CO} = 0.10$ cm-am, i.e. $q_{CO} = 4.8 \times 10^{-4}$, assuming uniform mixing. Given the sensitivity of the models to the CO abundance – and the small impact of thermal profile uncertainties (Table 1) – the allowed range is $q_{CO} = 5^{+10}_{-2.5} \times 10^{-4}$. Although the S/N of the Pluto spectrum is considerably lower than that for Triton (Lellouch et al. 2010), the accuracy on the CO abundance is comparable. This stems from the fact that the Pluto CO lines are instrinsically less narrow and saturated than their Triton counterparts, given the higher gas temperature (~90 K vs. ~50 K) and ~4 times smaller CO column density on Pluto vs. Triton.

Table 1. Best fit CH_4 and CO abundances vs. surface pressure.

Pressure	CH_4		CO	
(μbar)	Col. dens.	Mixing ratio	Col. dens.	Mixing ratio
6.5	0.6 cm-am	6.0×10^{-3}	0.07 cm-am	7.0×10^{-4}
15	1.2 cm-am	5.7×10^{-3}	0.10 cm-am	4.8×10^{-4}
24	1.7 cm-am	5.3×10^{-3}	0.14 cm-am	4.4×10^{-4}

A similar line coaddition process can be performed on the CH_4 lines. However, the larger complexity of the methane spectrum implies some a priori selection of the CH_4 lines. An example is shown in the right panel of Fig. 2, using the twelve CH_4 features marked in Fig. 1. The "combined CH_4 line" is then detected at ~11-σ. With $CH_4/N_2 = 0.6\%$, the CH_4/CO ratio in Pluto's atmosphere is nominally equal to 12, but could be in the range 2–48 for the CH_4 determined in this study, or 2.5–24 if the more precise value $q_{CH_4} = 0.5 \pm 0.1\%$ is used.

4. Discussion

The CO amount we infer is much smaller than values previously reported. Using the same CO(2–0) band and IRTF/CSHELL, Young et al. (2001) obtained a thermal-profile dependent upper limit $a_{CO} < (1.2\text{–}3.5) \times 10^{21}$ cm^{-2}, i.e. <45–130 cm-am. This limit was improved by ~2 orders of magnitude from our VLT/CRIRES observations of the CO(3–0) band ($a_{CO} <$ 1 cm-am, Lellouch et al. 2010), but the present CO determination is another factor-of-10 lower. At millimeter wavelengths. Bockelée-Morvan et al. (2001) obtained a tentative (formally 4.5σ) detection of the CO(2–1) line at 1.3 mm, using the IRAM 30-m telescope, that, if real, would indicate a CO/N_2

mixing ratio in the 1.2–7% range (also thermal-profile dependent). However, it was more cautiously interpreted as an upper limit, due to strong galactic contamination in their Pluto spectrum. The associated CO column was <3–7 cm-am, over a factor of 6 more constraining than the Young et al. (2001) results. The present evidence for CO suggests that the authors were indeed wise to regard their result as an upper limit.

Pluto's surface pressure reflects sublimation equilibrium for N_2 ice, and N_2 may follow saturation in a putative Pluto troposphere. Yet, the large CH_4 mixing ratio at ~90 K in Pluto's stratosphere implies that it is not severely affected by atmospheric condensation, and that if Pluto has a troposphere, strong supersaturation of CH_4 occurs (Lellouch et al. 2009). Rannou & Durry (2009) reached the same conclusion from microphysical arguments, but also mentioned that N_2 and CO can easily condense. Given its equilibrium vapor pressure, only a factor of ~8 lower than N_2 at 37 K, a ~0.05% CO/N_2 mixing ratio implies instead that CO condensation does not occur.

As first pointed out by Lellouch (1994), CO is a cooling agent in Pluto's atmosphere through radiation in its pure rotational lines, but its importance has been initially overstated. Lellouch found that when CO cooling was included in the Yelle and Lunine thermal model (1989) – that included absorption in the 3.3 μm band of CH_4 as the only energy source – the ~100 K stratospheric temperature required a very large (>10%) CH_4 abundance. Strobel et al. (1996) showed that this requirement was relaxed to ~3% when heating in the 1.6 and 2.3 μm CH_4 bands was considered. Still, in the presence of CO, a slightly negative temperature gradient (mesosphere) is expected in the sub-microbar region, evidence for which was claimed in occultation-derived thermal profiles (Elliot et al. 2007). However, the recent analysis by Zalucha et al. (2011) did not confirm the need for CO to explain occultation data. These authors directly modelled occultation light-curves with physically-based thermal profiles calculated from a radiative-conductive model inherited from Strobel et al. (1996), and in which the surface pressure and the CH_4 and CO mixing ratios are free parameters. Zalucha et al. (2011) deduced CH_4 mixing ratios of 0.18–0.94% for occultations recorded in 1988, 2002, 2006, and 2008 (albeit with no specific trend with time), broadly consistent with the observed ~0.5% mixing ratio. In contrast, and although they confirmed that CO does affect the thermal structure in the μbar region (see e.g. their Fig. 8), their simulations indicated that occultation lightcurves are essentially insensitive to the CO mixing ratio. As a further testimony of the less than originally thought importance of CO for controlling Pluto's atmosphere state, Strobel (2008) found that CO plays at most a minor role in the atmospheric escape rates.

Our inferred atmospheric CO mixing ratio is consistent with the long-standing predictions by Owen et al. (1993), Lellouch (1994) and Strobel et al. (1996). These estimates, which spanned the range $(2–20)\times10^{-4}$, were obtained assuming an ideal N_2–CO–CH_4 solid solution (Raoult's law) and using the then available CO/N_2 ice mixing ratio (0.5%, from Owen et al.). However a refined analysis of the near-IR spectra indicates that CO is present on Pluto's surface with a mixing ratio of 0.08–0.2% relative to N_2 (Douté et al. 1999). Using modern vapor pressure data (Fray et al. 2010), the ideal mixture case leads to an atmospheric CO/N_2 of $(1.0–2.7)\times10^{-4}$, only marginally in agreement with the observed $(2.5–15)\times10^{-4}$ range. Rather, the atmospheric and surface CO/N_2 mixing ratios are the same within error bars, a situation predicted by the "detailed balanced" model (Trafton 1990; Trafton et al. 1998). In this scenario, surface-atmosphere exchanges in presence of escape and seasonal transport lead to an atmospheric composition reflecting that of the accessible ice reservoir from which it is replenished. In the case, relevant for a CO/N_2 mixture, where no fractionation occurs during escape or transport, the process equalizes the mixing ratios in the atmosphere and the volatile reservoir. This is made possible by the formation of a thin CO-enriched surface veneer in equilibrium with the atmosphere according to Raoult's law. Lellouch et al. (2010) found this scenario to be valid for CO on Triton.

The alternative scenario would be that the enhanced CO abundance compared to the ideal solution case results from the presence of pure CO patches. The CO partial pressure is 4–25 nbar, i.e. 80–500 times less than the vapor pressure of pure CO. Hence, patches of pure CO covering 0.2–1.2% of Pluto's surface could in theory produce the elevated CO abundance. Problems with this scenario are that (i) the formation of pure CO grains is not expected thermodynamically, given the complete miscibility of N_2 and CO (ii) CO is not buoyant in N_2, inhibiting the sublimation of any CO patch (Stansberry et al. 1996). Yet, the longitudinal distribution of the CO 1.58 μm ice features shows evidence for a CO-rich region near longitude $L = 180°$ (Grundy & Buie 2001), which (coincidentally or not) corresponds to the brightest and least red region in HST maps near Pluto's equator (Buie et al. 2010). This situation contrasts with the Triton case, where the longitudinal distributions of the N_2 and CO ice bands are remarkably similar (Grundy et al. 2010). How could CO become concentrated in a localized spot on Pluto remains to be elucidated. Hopefully, combined imaging and spectroscopy from New Horizons will reveal the nature of this CO-rich region and whether it may contribute to the CO atmospheric abundance.

Acknowledgements. This work is based on observations performed at the European Southern Observatory (ESO), proposal 085.C-0113.

References

Bockelée-Morvan, D., Lellouch, E., Biver, N., et al. 2001, A&A, 377, 343
Buie, M. W., Grundy, W. M., Young, E. F., et al. 2010, AJ, 139, 1128
Cruikshank, D. P., Roush, T. L., Moore, J. M., et al. 1997, in Pluto and Charon, ed. S. A. Stern, & D. J. Tholen (The University of Arizona Press), 221
Douté, S., Schmitt, B., Quirico, E., et al. 1999, Icarus, 142, 421
Elliot, J. L., Person, M. J., Gulbis, A. A. S., et al. 2007, AJ, 134, 1
Fray, N., & Schmitt, B. 2010, Planet. Space. Sci., 57, 2053
Grundy, W. M., & Buie, M. W. 2001, Icarus, 153, 248
Grundy, W. M., & Buie, M. W. 2002, Icarus, 157, 528
Grundy, W. M., Young, L. A., Stansberry, J. A., et al. 2010, Icarus, 205, 594
Käufl, H. U., Ballester, P., Biereichel, P., et al. 2004, SPIE, 5492, 1218
Lellouch, E. 1994, Icarus, 108, 225
Lellouch, E., Sicardy, B., de Bergh, C., et al. 2009, A&A, 495, L17
Lellouch, E., de Bergh, C., Sicardy, B., Ferron, S., & Käufl, H.-U. 2010, A&A, 512, L8
Merlin, F., Barucci, M. A., de Bergh, C., et al. 2010, Icarus, 210, 930
Olkin, C. B., Elliot, J. L., Hammel, H. B., et al. 1997, Icarus, 129, 178
Owen, T. C., Roush, T. L., Cruikshank, D. P., et al. 1993, Science, 261, 745
Protopapa, S., Boehnhardt, H., & Herbst, T. M. 2008, A&A, 490, 365
Rannou, P., & Durry, G. 2009, J. Geophys. Res., 114, 11013
Stansberry, J. A., Spencer, J. R., Schmitt, B., et al. 1996, Planet. Space Sci., 44, 1051
Strobel, D. F. 2008, Icarus, 193, 612
Strobel, D. F., Zhu, X., & Summers, M. E. 1996, Icarus, 120, 266
Trafton, L. M. 1990, ApJ, 359, 512
Trafton, L. M., Matson, D. L., & Stansberry J. A. 1998, in Solar System Ices, ed. B. Schmitt, C. de Bergh, & M. Festou (Kluwer Academic Publishers), 773
Yelle, R. V., & Lunine, J. I. 1989, Nature, 399, 288
Young, L. A., Elliot, J. L., Tokunaga, A., de Bergh, C., & Owen, T. 1997, Icarus, 127, 258
Young, L. A., Cook, J. C., Yelle, R. V., & Young, E. F. 2001, Icarus, 153, 148
Zalucha, A. M., Gulbis, A. A. S., Zhu, X., et al. 2011, Icarus, 211, 804